Effects of Thermal Expansion Mismatch on Solid Breeder Blanket Pebble Bed and Structural Clad Thermomechanics Interactions

A. Y. Ying, H. Huang, M. A. Abdou
Mechanical & Aerospace Engineering Department,
UCLA, Los Angeles, CA 90095
310-206-8815
ying@fusion.ucla.edu

L. Zi
Jaycor, San Diego
858-623-3720
zlu@jaycor.com

ABSTRACT

In this paper, a thermomechanical interaction of a ceramic breeder pebble bed and structural plate is studied based on a recently developed discrete numerical simulation code. The calculations take into account the coupling effect between structural wall deformation and pebble bed deformation, which greatly increases the computing time and complicates the computational procedures in determining the particle-wall contact characteristics. Specifically, the model is applied to a lithium orthosilicate packed bed for the evaluation of the deformation of a circular plate due to bed thermal expansion, while the results are compared with SCATOLA's experimental data. Numerical results using a fixed boundary condition show reasonable agreement with the experimental data. In addition, numerical simulations confirm an irreversible plate deformation after a thermal cycle run as observed in the experiments, although these experimentally observed deformations are larger than that of the numerical estimations. Moreover, numerical results of contact forces at contact points provide information concerning the mechanical integrity of the bed at a moderately high temperature.

I. INTRODUCTION

Solid breeder blanket concepts are typically based on the use of pebble beds of lithium ceramics as a breeder material and of beryllium as a neutron multiplier. During reactor operation, the bed will undergo thermal expansion relative to the container due to higher expansion coefficient in comparison with that of the surrounding structure, their substantial temperature differences, and/or the irradiation swelling of particles, which will cause stresses. These stresses may break the particles and endanger safe blanket operation, particularly if heat and tritium removal significantly deteriorate due to ceramic particle breakage. Consequently, the determination of these stresses is important in the design of a solid breeder blanket.

At present, there are a number of on-going investigations into the thermomechanical behavior of ceramic breeder and beryllium pebble-beds by experimental and computational methods[1-2]. Main features of the observed pebble beds behavior are non-linear elastics, partially irreversible deformation due to compaction, and creep effects. Unfortunately, many behaviors of particles and among particles are very difficult to describe in detail and precisely due to the discrete nature of a pebble bed system based only on macroscopic experiments or continuum numerical methods. On the other hand, the application of commercial numerical tools to simulate a prototypical blanket pebble bed operation does not occur easily, while consecutive equations obtained from the experimental data as well as extension of the model for bed rearrangement are unavoidable.

A numerical model based on a discrete scheme is more flexible in its application. It can provide microscopic insights into thermal-mechanical interactions, as well as particle relocations. The objective of this paper is to modify a previously developed 3-D discrete numerical simulation model[3] to predict the stress levels and consequent container deformations of a typical fusion blanket pebble bed under high temperature operations. This modified program then serves as a basis for further determination of thermal creep behavior. The calculations take into account the coupling effect between structural wall deformation and pebble bed deformation, which greatly increases the computing time and complicates the computational procedures in determining the particle-wall contact characteristics. The model is applied to a lithium orthosilicate packed bed for the evaluation of the deformation of a circular plate due to bed thermal expansion, while the results are benchmarked with SCATOLA's experimental data[4].

II. MATHEMATICAL MODEL

In a discrete numerical simulation, the elastic phenomenon of a particle bed is modeled as a collection of rigid particles interacting via Mindlin-Hertz type

contact interactions[5-7]. Under zero load, the particles are in contact at a single point. As the load is imposed, the particles deform in the vicinity of the point of initial contact, such that the contact area will be finite (though small compared to particle size). The detection of contacts between two particles is done in a straightforward fashion, where the distance between the origins of any two vicinity particles are checked for overlap.

Under a quasi-static condition, the force acting on any particle leading to the equation of motion reduces to the following equilibrium conditions

$$\mathbf{F} - \sum_c \mathbf{F}_c = 0 \tag{1}$$

where F is the externally imposed force and the summation is performed over the contacts of the particle. At equilibrium, each particle in the assembly should satisfy the above equation.

If the particle is not at the equilibrium, the particle is subjected to displacement according to the active force and bed stiffness. In the model, the degree of particle movement/displacement in response to environmental change is described by the action of springs virtually attached at 3 coordinates in the x, y and z planes. As shown in Figure 1, the particle is displaced according to the stiffness (K_n and K_s) of the contacts with neighboring particles. The relationship between the force and displacement is estimated based on[6],

$$F_n = k_n \delta_n \tag{2}$$

$$F_s = k_s \delta_s \tag{3}$$

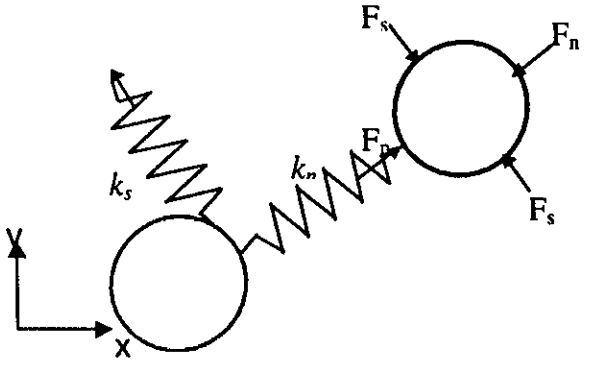

Figure 1 Representation of the force-displacement relation at contact between two particles

where the normal force at the contact F_n is expressed by Hertz theory as[5]:

$$F_n = \frac{4E^* \sqrt{R\delta^3}}{3} \tag{4}$$

and shear force which is proportional to shear displacement at each contact and the shear stiffness as given in [6-7]

$$\Delta F_s = k_s \Delta u_s \tag{5}$$

and

$$k_s = \frac{2G^{2/3}[6(1-\nu)RF_n]^{1/3}}{2-\nu} \tag{6}$$

In addition, the friction at an interface is described using Coulomb's friction law[9] that states that at incipient sliding, the friction force is given by

$$F_f = F_n \tan\phi_\mu = F_n k_f \tag{7}$$

where ϕ_μ is the interface friction angle, and k_f=tanϕ_μ is the friction coefficient.

Numerically, the contact forces (normal, shear or friction forces) are decomposed into x, y, z components based on the unit vector evaluated from the centers of the two contacted particles. The incremental displacement of the particle in the x-direction is derived based on the net active force along the x-axis according to:

$$\Delta D_x = \frac{F_x}{k_t} = \frac{\sum_c F_{xc}}{k_n + k_s}$$

$$for, \frac{k_s}{k_n + k_s} \left| \sum_c F_{xc} \right| < k_f \sqrt{(\sum_c |F_{yc}|)^2 + (\sum_c |F_{zc}|)^2},$$

otherwise

$$\Delta D_x = \frac{F_x - k_f |F_t|}{k_n} = \frac{\sum_c F_{xc} \pm k_f \sqrt{(\sum_c |F_{yc}|)^2 + (\sum_c |F_{zc}|)^2}}{k_n} \tag{8}$$

The ± signs in the above equation should be chosen such that the friction forces are opposite to the active force. Similar expressions can be written for the displacements in the y and z directions.

In equation 8, the stiffness k_n of the relaxation spring still needs to be determined. It is related to the normal contact force of two touching particles in equation (4). To simplify the computation, a least-square regression method is used to approximate the Hertz nonlinear relationship to a linear equation. The resultant best estimation for bed stiffness in the normal direction gives:

$$k_n = \frac{8E^* \sqrt{R\delta_f}}{7} \tag{9}$$

where δ_f is the maximum value among all δ_c at particle contact points.

The program generates an initial particle assembly for a single size bed. As input data, the total particle number, the thermal and mechanical properties of solid particle materials, and the particle size distribution are required. The sizes of the assembly volume and the minimal and maximal particle radii and their position coordinates are calculated and/or recorded during the assembly generation process, respectively. Large stresses may be exerted on each container wall, and among particles due to overly packed and a high initial packing density. The program slowly expands the container to release the stresses exerted on it, as well as reduce the particle overlaps, until the final stress is less than 3.0×10^{-4}MPa to complete the initial packing. Numerically, prototypical packing densities of about 60-62%, depending on the particle size (large or small) and the particle size distribution (e.g. Gaussian distribution), are achieved. Additional details of this numerical model can be found in Reference 1.

III. SCATOLA SIMULATION

One of this paper's objectives is to apply the aforementioned numerical code to predict and compare with the experimental data of SCATOLA - a cylindrical pebble bed thermomechanical test assembly (see Figure 2). The ceramic lithium orthosilicate pebbles are enclosed between two plates that are fixed at their circumference. In the experiment, the relative movements of the top and bottom plates, with respect to temperature rises, are measured. Further description of this test can be found in Reference 2.

Initially, the previously developed code is modified to a cylindrical coordinate system taking into account the SCATOLA experimental setup. As the pebble bed temperature rises, the particle overlap at the contact point due to thermal expansion is calculated as:

$$\delta = R_i(1+\alpha\Delta T_i) + R_j(1+\alpha\Delta T_j) - D_{ij} \tag{10}$$

where D_{ij} is the distance between particle i and particle j along the normal direction prior to thermal expansion. Under a constrained bed thermal expansion, the difference in coefficients of thermal expansion between the pebble and plate will produce thermal stress under a uniform temperature rise. This plate deformation by differential thermal expansion (produced by thermal stress due to

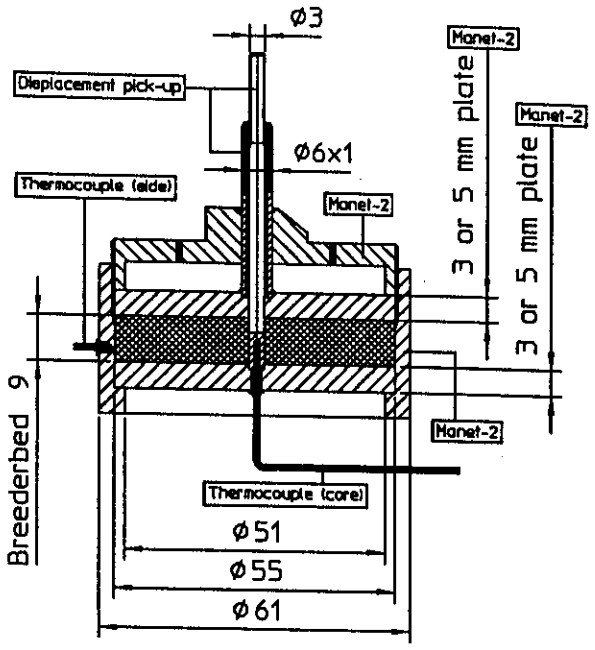

Figure 2 Details of SCATOLA Test Apparatus

particle temperature rise) depends on the boundary conditions. Analytical solutions of plate deformations under uniform pressure (with respect to the simply supported and fixed boundary conditions) are formulated in the code as follows[10]:

$$W^*_{d\ supported} = \frac{\sigma_{th}}{64D}\frac{5+\nu}{1+\nu}a^4 \tag{11}$$

under simply supported boundary condition or

$$W^*_{d\ fixed} = \frac{\sigma_{th}}{64D}a^4 \tag{12}$$

with fixed boundary condition. The total thermal expansion of the plate is given as:

$$W = W_{uniform} + W^*_d \tag{13}$$

where the uniform thermal expansion of container or the axial displacement in z direction is given by:

$$W_{uniform} = \alpha_w * \Delta T * h \tag{14}$$

where h is height of cylinder container.

Numerically, two iterative loops are set-up to calculate a self-consistent force and displacement

relationship. The first iterative loop searches for an equilibrium pebble bed configuration with respect to particle relocation due to a temperature rise. The second iteration defines the new container boundary based on the calculated plate deformation value caused by the stress exerted on the plate. It is noted that an exact simulation requires modeling a large number of particles. For example, considering an average diameter of 0.44 mm that is being used in the experiments (to cover the range of particle sizes from 0.25 to 0.6 mm), the simulation requires the use of ~ 323,750 particles. To remedy this, parametric studies were conducted to evaluate the effect of particle sizes on bed/clad thermomechanical interaction. Numerical results for 1 mm size particle (total number of particles ~ 26,010) and 2 mm size particle (3,072) beds have shown that the stress exerted on the wall, and therefore the plate deformation for a deformable boundary, is less sensitive to the particle sizes[9]. Consequently, it is believed that the thermomechanical behavior of SCATOLA experiments is adequately simulated using 26,010 1-mm particles.

IV. RESULTS

A. SCATOLA Simulation

The packing characteristic for the bottom layer of the packing in a quarter plane is shown in Figure 3. This packing structure is similar to that of the experimentally observed orthorhombic packing for a single size bed. It gives a typical initial packing density of about 61.6 %. In addition, an enlarged view of particle locations at 600 °C relative to that at the room temperature is show in Figure 4. It is noted that the particles have slightly shifted and displaced to reflect the bed thermal expansion due to a temperature increase.

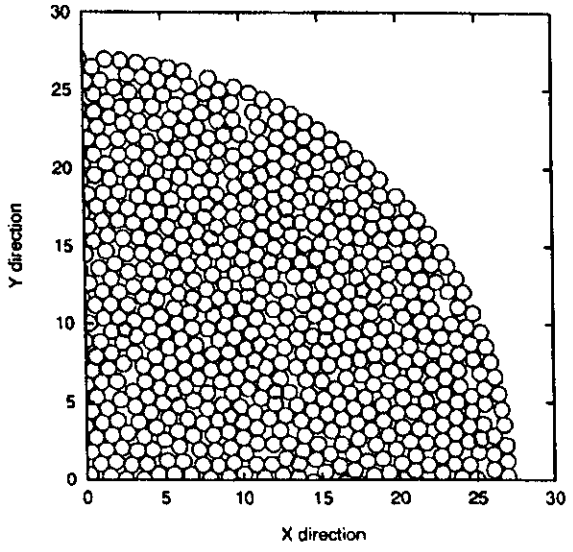

Figure 3 Packing characteristics of the bottom layer of packing (mean particle diameter = 1 mm total number of particles = 26,010)

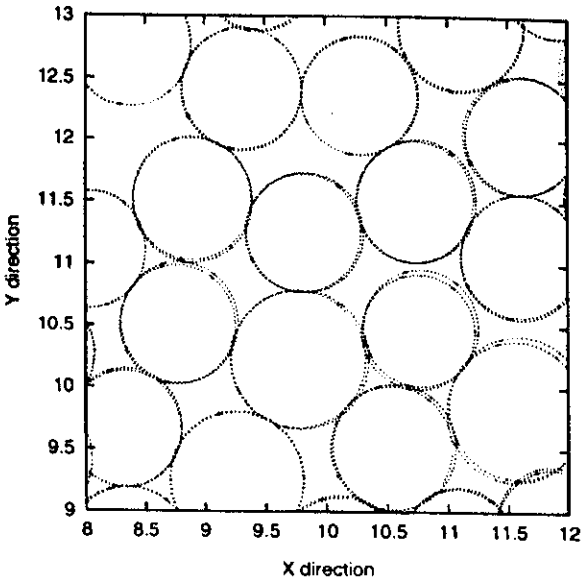

Figure 4 Enlarged view of particle relocations due to constrained bed thermal expansions (Relative locations of particles at room temperature and at 600 °C are shown)

The average stress exerted on the plate under the equilibrium condition as a function of temperature increase is shown in Figure 5. This stress produced by thermal differential expansion, up to 7 MPa, causes the plate to deform and results in a maximum deformation located at the center. The estimations indicate that the deformation depends on the boundary conditions and the initial packing states. The deformation increases if an initial-residual stress exists in the bed[9]. The deformation is higher under a simply supported boundary condition as compared to that of the fixed boundary condition. Numerical results show that the experimental deformation data falls between that of the calculated results with simply supported and with fixed boundary conditions as shown in Figure 6 and, that it is much closer to the predictions based on the fixed boundary condition as shown in Figure 7. This appears reasonable since the imposed boundary condition in the experimental set-up lies somewhat between the aforementioned two boundaries (namely simply supported and the fixed boundaries), while the circumference of the plate was fixed. In addition, numerical simulations confirm an irreversible plate deformation after a thermal cycle run as observed in the experiments. However, these experimentally observed deformations are larger than that of the numerical estimations (whereas, a larger deformation was observed for a thinner plate). This

deformation, which may be caused by the residual stress inside the bed, particles being locked inside the bed, and/or other unclear reasons, is thus not yet simulated adequately.

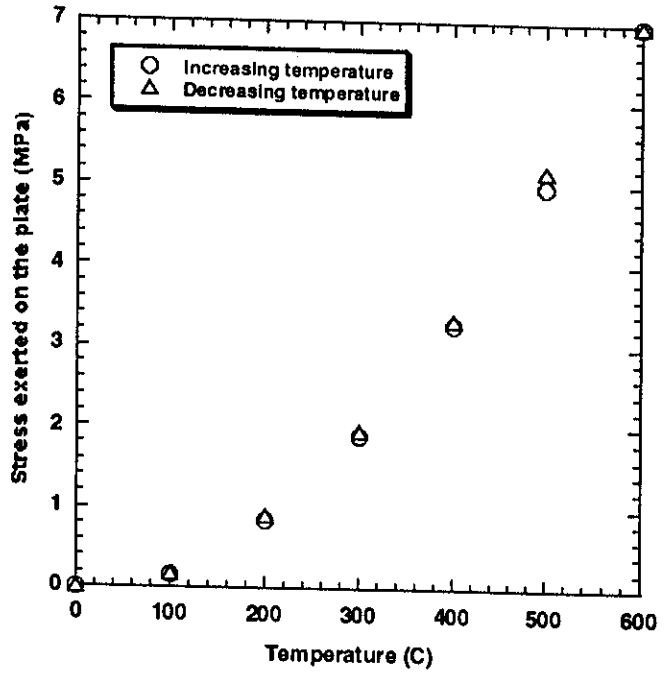

Figure 5 Calculated stresses exerted on the plate due to differential thermal expansion between pebble and structural materials

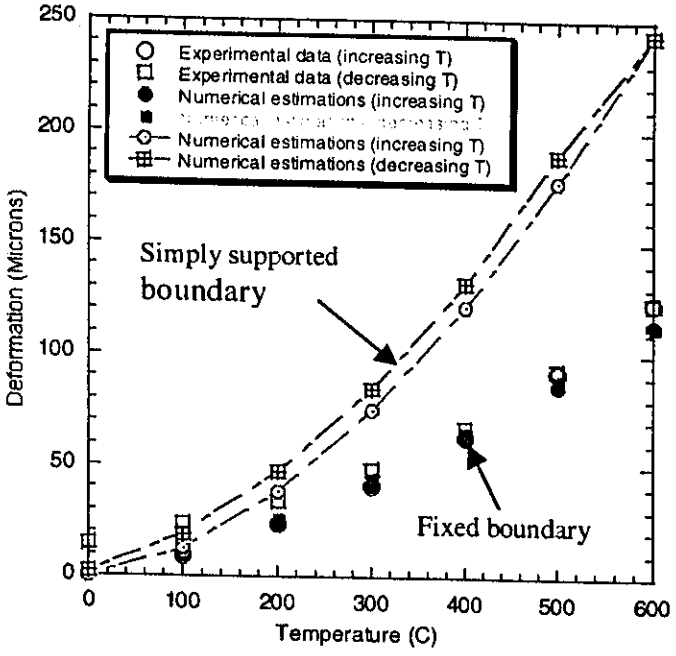

Figure 6 Experimental deformation falls between that of calculated results with simply supported boundary and with fixed boundary conditions (for a plate thickness of 5.5 mm)

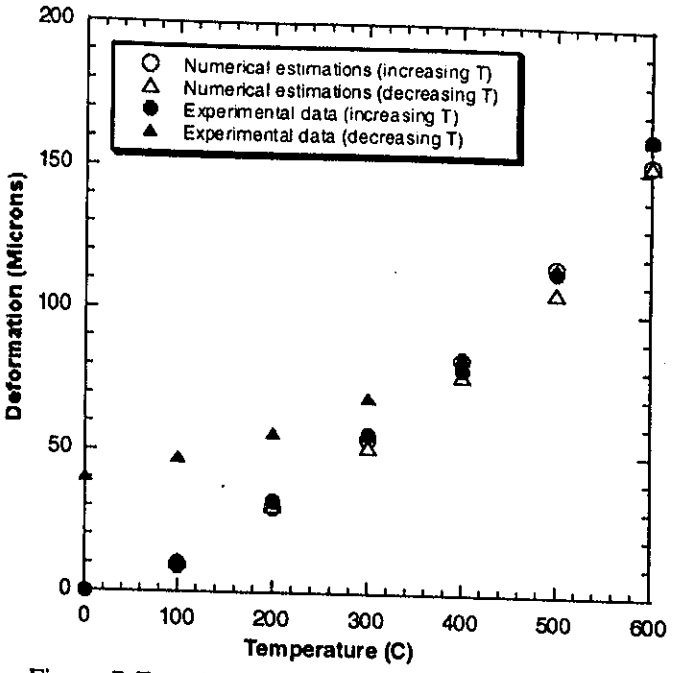

Figure 7 Experimental data are reasonably predicted by the numerical estimations based on fixed boundary conditions.

B. Contact Force Distribution

The discrete numerical simulation provides detailed information with respect to contact characteristics. These include contact areas and contact forces at the contact between any two contacted surfaces (among particles and between particles and wall). One of the parameters of interest concerns the contact force as compared to the crush load of the particle material. To illustrate this feature, a contour plot of the forces that are exerted on the particle at the contact in contacting the bottom of the container is shown in Figure 8. This plot helps identify where and how many particles will break under a compressive stress that results from the differential thermal expansion and particle relocations. As shown, three over about 400 particles are under a compressive force of greater than 125 N (the crush load for the Li_4SiO_4 pebble) at 600 °C. A 3-D plot indicating all particles that may break due to a constrained thermal expansion is shown in Figure 9. As shown, twenty-four particles are found to break due to a large compressive force at the contact. This information provides the designer with the mechanical integrity of the bed and insight into pebble behavior.

V. SUMMARY

The stress magnitude exerted on the plate, consequent container plate deformation, and bed elastic

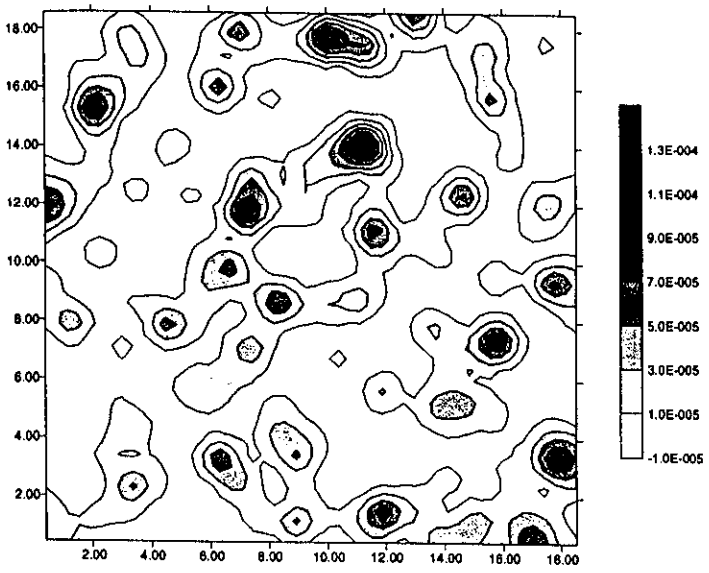

Figure 8 Contour plot of contact forces at the wall and particle contacts (Unit: MN)

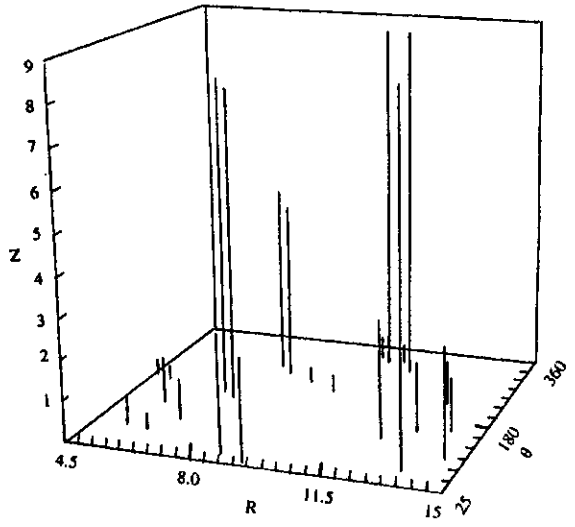

Figure 9 Numerical simulation shows that twenty-four particles are found to break due to a large compressive force at the contact that results from the differential thermal expansion and particle relocations. Tip of the vertical line indicates the center of the particle and, the vertical line is used to help illustrate the location of the particle. (R and z units: mm; total number of particles=9000)

properties under moderate high temperature (up to 600 °C) operations are estimated using a 3-D discrete micro-thermomechanics model. The behavior of a particle bed in the elastic regime is modeled as a collection of rigid particles interacting via a Hertz-Mindlin type contact. The model tackles the incremental movements of the constrained particles, which are caused by temperature increases. Specifically, simulations are performed for a prototypical SCATOLA cylinder container with slightly larger particles (total number of 1 mm diameter particles = 26,010). Numerical calculations show reasonable agreement with observations from experiments. The estimations indicate that the deformation depends on the boundary conditions. The deformation is higher under a simply supported boundary condition. Experimental data falls between that of the calculated results with simply supported and with fixed boundary conditions, and compared reasonably well with that of the numerical estimations with a fixed boundary condition. Furthermore, the discrete numerical simulation provides detailed information with respect to contact characteristics. Present calculations show that a small percent (~ 0.26%) of particles are found to break due to a large compressive force at the contact that results from the differential thermal expansion and particle relocations.

After a complete thermal cycle, a portion of the deformation of packed beds that may be caused by the residual stress inside the bed and/or particle rearrangements is found numerically, although experimental observations are higher. On the other hand, it has also been shown that at temperatures higher than 650 °C, thermal creep occurs inside the bed. Thus, further development of this code needs to more accurately take into account plastic deformation, as well as thermal creep phenomena.

NOMENCLATURE

a = plate radius

$$D = \frac{Et^3}{12(1-\nu^2)}$$

E = *Young's modulus*

$$\frac{1}{E^*} = \frac{1-\nu_1^2}{E_1} + \frac{1-\nu_2^2}{E_2}$$

G = *elastic modulus*
h= *height of cylinder container*
k= *stiffness*
R = *radius of particle*
t= *plate thickness*
T= *Temperature*

Greek
α = *thermal expansion*
ν = Poisson's ratios
σ = thermal stress
δ = deformation, displacement

Subscripts
c= contact
n= normal
th= thermal
s= shear
x,y,z = coordinates
w= wall container
1,2 = particle number

ACKNOWLEDGEMENT

This work was performed under U.S. Department of Energy Contract DE-FG-03-86ER-52123.

REFERENCES

1. L. Bühler, "Elasticity of granular materials in fusion breeding blankets" in: Proceedings of the 20th SOFT (1998), pp. 1345-1348.

2. J. Reimann, E. Arbogast, M. Behnke, S. Müller and K. Thomauske: "Thermomechanical behaviour of ceramic breeder and beryllium pebble beds", presented at ISFNT-5, Rome, Sep. 1999, to be appeared in Fusion Engineering and Design

3. Lu Zi, Numerical and Experimental Measurement of the Thermal and Mechanical Properties of Packed Beds, Ph. D. Thesis, UCLA, June, 2000

4. J. G. van der Lann et al., Thermomechanical Behavior of HCPB Pebble-Bed Assemblies in SCATOLA Experiments and Design Analyses for Irradiation in HFR, Proceedings of CBBI-8, October, 1999 (Available upon request).

5. Johnson, K.L. (1985), Contact Mechanics, Cambridge University Press, London.

6. Mindlin, R.D. (1949), Compliance of elastic bodies in contact, Journal of Applied Mechanics, Vol. 16, 259

7. Mindlin, R.D. and Deresiewicz, H. (1953), Elastic spheres in contact under varying oblique forces, Journal of Applied Mechanics, Vol. 20, 327

8. Kishino, Y. (1988), Disc model analysis of granular media, in: M. Satake and J.T. Jenkins, eds., Micromechanics of Granular Materials, Elsevier, Amsterdam, pp. 143-152.

9. Singer, I.L. and Pollock, H.M. (1992), Fundamentals of Friction: Macroscopic and Microscopic Processes, Klumwer Academic, Dordrecht, The Netherlands.

10. T. H. Hsu, Stress and Strain Data Handbook, pp. 173-182, Gulf Publishing Company, 1986

11. L. Zi, A. Ying, H. Huang, M. Abdou, Effects of Thermal Expansion Mismatch on Pebbled Bed/Clad Thermomechanical Interactions: Progress on SCATOLA Simulation Study, Presented at CBBI-9, NIFS, Sep. 2000.